View metadata, citation and similar papers at core.ac.uk
brought to you by CORE
provided by Infoscience - École polytechnique fédérale de Lausanne

Optical emission spectroscopy to diagnose powder formation in SiH_4-H_2 discharges

B. Strahm, A. Feltrin, R. Bartlome & C. Ballif

Ecole Polytechnique Fédérale de Lausanne (EPFL), Institute of Microengineering IMT, Photovoltaics and thin film electronics laboratory, Breguet 2, 2000 Neuchâtel, Switzerland.

ABSTRACT

Silane and hydrogen discharges are widely used for the deposition of silicon thin film solar cells in large area plasma-enhanced chemical vapor deposition reactors. In the case of microcrystalline silicon thin film solar cells, it is of crucial importance to increase the deposition rate in order to reduce the manufacturing costs. This can be performed by using high silane concentration, and usually high RF power and high pressure, all favorable to powder formation in the discharge that generally reduces the deposition rate as well as the deposited material quality. This work presents a study of powder formation using time-resolved optical emission spectroscopy. It is shown that this technique is suitable to detect different regimes in powder formation ranging from powder free discharge to discharge producing large dust particles. Intermediate powder formation regimes include the formation of small silicon clusters at plasma ignition as well as cycle of powder growth and ejection out of the discharge, and both are observable by this low-cost and experimentally simple technique.

Optical emission spectroscopy, silane-hydrogen discharge, powder formation

1. INTRODUCTION

Cost reduction is a major issue in silicon thin film solar cells manufacturing to compete with conventional electricity sources. Therefore, the development of new processes as well as new equipments is mandatory to enable an increase in deposition rates over large areas (> 1 m^2). This is of major importance in the case of micromorph cells, combining a thin top amorphous silicon cell and a thick bottom microcrystalline silicon cell. Indeed, one of the most expensive parts in such cells is the microcrystalline silicon layer because of its important thickness (≈ 2 µm), making the processing time very long for standard deposition rates (< 0.5 nm/s) using plasma-enhanced chemical vapor deposition (PECVD) with silane (SiH_4) and hydrogen (H_2) as source gases.
Increase in the deposition rate for microcrystalline processes is achieved mainly by playing with the deposition parameters. The RF power [1], the SiH_4 concentration in H_2 [2], as well as the working pressure [3] have been increased to achieve higher SiH_4 dissociation efficiency to raise the deposition rate. However, all three techniques, even separately, have the notable drawback to increase the powder formation in the discharge. Powder formation starts by the appearance of poly-silanes (Si_2H_6, Si_3H_8,…) resulting from the gas phase reaction of the SiH_2 silane radicals [4] or anions [5] issued form silane dissociation in the plasma with undissociated silane. Once these poly-silanes formed, they lead rapidly to coarser silicon particles associated to powder [6]. Therefore, the techniques to increase the silane dissociation efficiency consisting in increasing the silane dissociation rate by increasing the RF power density or increasing the silane residence time in the plasma by increasing the pressure or the silane concentration lead all to powder formation by promoting the poly-silanes generation.

Therefore, the detection of the onset of powder formation is of crucial importance in order to find the optimum deposition parameters, balanced between the beneficial effect of the increase in RF power, pressure and silane concentration on the deposition rate and powder formation in the discharge. Different techniques have been proposed to detect powder formation such as electrical characterization of the discharge [5], laser light scattering [7] or mass spectroscopy [8]. In this work, optical emission spectroscopy is proposed to detect the powder formation in silane-hydrogen discharges. It is shown that this low cost and experimentally simple technique allows the detection of electron density as well as electron temperature perturbation by the presence of powder compared to steady-state discharge in powder free regimes.

Section 2 introduces the experimental basis for the acquisition and data treatment of time-resolved optical emission spectra. The different effects of particles/powder on the emission spectra are presented in Section 3.1. The effect of an increase in working pressure on the powder formation and detection by OES is discussed in Section 3.2.

2. EXPERIMENTAL ARRANGEMENT

The deposition reactor used in this work was a KAI-M reactor manufactured by Oerlikon-Solar AG. This large area Plasma-Box type reactor has a showerhead RF electrode that guarantees uniform gas and power distribution. Gas precursors for silicon thin film deposition were silane (SiH_4) and hydrogen (H_2).
Time-resolved optical emission spectroscopy (OES) was used to diagnose the plasma emission. Acquisitions were made from a view-port installed on the lateral side of the deposition reactor. The light was guided from the view port through a UV/VIS optical fiber to the spectrometer (Ocean Optics USB2000+). Acquisitions were started prior to plasma ignition with an integration time of 25 ms. Emissions resulting from molecular (Fulcher and G_0B_0) and atomic (H_α and H_β) hydrogen detailed in Tab. 1 were integrated after dark noise subtraction. Silane emission was monitored by integrating the SiH emission line after dark and hydrogen background subtraction following the method detailed by Howling *et al* in Ref. [9].

Line/band	Source	Wavelength (nm)
H_α	$e^- + H_2$	656.2
	$e^- + SiH_4$	
H_β	$e^- + H_2$	486.1
	$e^- + SiH_4$	
H_2 Fulcher	$e^- + H_2$	595-630
H_2 G_0B_0	$e^- + H_2$	461-464
SiH	$e^- + SiH_4$	410-425

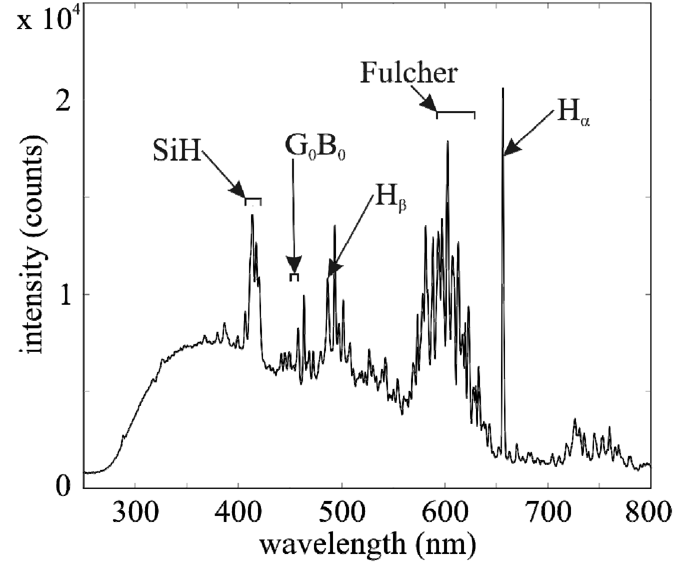

Figure 1: Optical emission line and spectrum for a typical SiH_4-H_2 discharge.

The time-dependent electron density was measured following the method presented in previous work [9]. It was calculated from the subtracted SiH emission intensity and the H_2 Fulcher integrated intensity that are given by

$$I_{\mathrm{SiH}}^{\mathrm{t}} = K_{\mathrm{SiH}} \cdot X_{\mathrm{SiH}}(T_{\mathrm{e}}) \cdot n_{\mathrm{e}}^{\mathrm{t}} \cdot n_{\mathrm{SiH_4}}^{\mathrm{t}} \tag{1}$$

and

$$I_{\mathrm{Ful}}^{\mathrm{t}} = K_{\mathrm{Ful}} \cdot X_{\mathrm{Ful}}(T_{\mathrm{e}}) \cdot n_{\mathrm{e}}^{\mathrm{t}} \cdot n_{\mathrm{H_2}}^{\mathrm{t}}, \tag{2}$$

respectively, where I_i^t are the time-dependent emission intensities, K_i constants accounting for collection, transmission and detection efficiencies of the emitted light, X_i the electron temperature dependent emission rate coefficient for electron impact excitation and n_i^t the time-dependent density of the *i* specie. The time-dependent electron density variation is therefore given by

$$\frac{n_{\mathrm{e}}^{t}}{n_{\mathrm{e}}^{0}} = \frac{I_{\mathrm{SiH}}^{t}}{n_{\mathrm{SiH_4}}^{t}} \cdot \frac{n_{\mathrm{SiH_4}}^{0}}{I_{\mathrm{SiH}}^{0}} = \frac{I_{\mathrm{SiH}}^{t}}{I_{\mathrm{SiH}}^{0}} \cdot \left[c + (1-c) \cdot \frac{I_{\mathrm{Ful}}^{t} I_{\mathrm{SiH}}^{0}}{I_{\mathrm{SiH}}^{t} I_{\mathrm{Ful}}^{0}} \right], \tag{3}$$

where *c* is the input silane concentration defined as the ratio of the silane flow rate to the total flow rate.
The electron temperature variation was qualitatively tested by the ratio of different emissions of molecular hydrogen [10]

$$\frac{I_{\mathrm{Ful}}^{t}}{I_{\mathrm{G0B0}}^{t}} = \frac{K_{\mathrm{Ful}} X_{\mathrm{Ful}}(T_{\mathrm{e}})}{K_{\mathrm{G0B0}} X_{\mathrm{G0B0}}(T_{\mathrm{e}})} \tag{4}$$

or atomic hydrogen

$$\frac{I_{\mathrm{H}\alpha}^{t}}{I_{\mathrm{H}\beta}^{t}} = \frac{K_{\mathrm{H}\alpha} X_{\mathrm{H}\alpha}(T_{\mathrm{e}})}{K_{\mathrm{H}\beta} X_{\mathrm{H}\beta}(T_{\mathrm{e}})}. \quad (5)$$

3. RESULTS AND DISCUSSION

This section presents and discusses the detection of powder formation by optical emission spectroscopy. First, the different effects of powder formation on the optical emission are reviewed. Second, measurements varying pressure with typical deposition parameters suitable for microcrystalline solar cell manufacturing are presented.

3.1 Zoology of powder effect on optical emission

Figure 2 presents two extreme cases of powder formation observation by optical emission spectroscopy (OES). Figure 2a presents the SiH and the H_2 Fulcher emission intensities for a discharge with a low silane concentration (1.25 %) and a low RF power input (300 W). The emission intensities do not vary in time because of the absence of poly-silanes/powder in this low power and low silane concentration case. On the other hand, Fig. 2b presents a chaotic behavior of the SiH and H_2 Fulcher emission intensities at ignition due to very strong powder formation. In this case the discharge parameters were 50 % of silane, a RF power input of 1000 W and a pressure of 6 mbar, all highly favorable to powder formation. These two extreme cases are the boundary of the present work and intermediate cases are discussed in the next paragraphs.

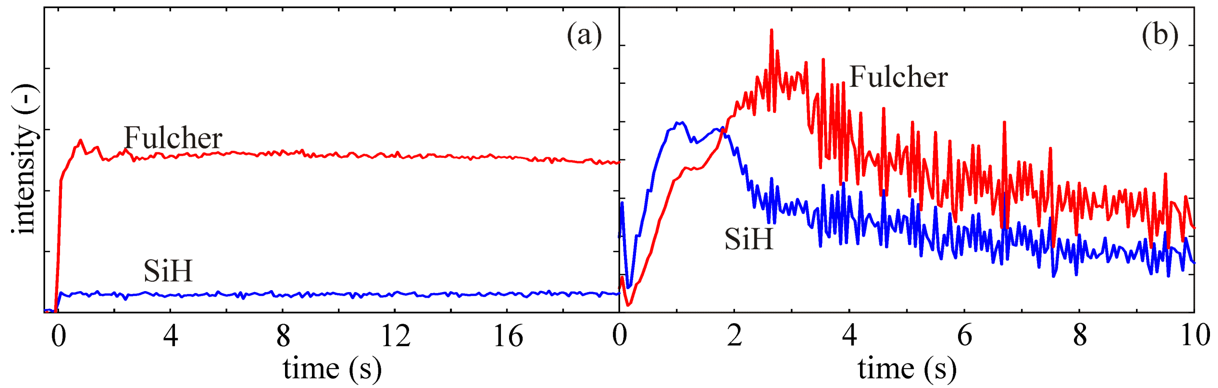

Figure 2: OES acquisitions at ignition of (a) a non-powdery discharge (6 mbar, 1.25%, 350 W) with constant emission intensities and (b) a powdery discharge (6 mbar, 50 %, 1000 W) with chaotic emission intensities.

Figure 3 presents OES acquisitions (emission intensities, electron density variation and hydrogen intensity ratio) performed with low silane concentration (5 %) and RF power (400 W) for two different pressures: 1.75 mbar (a) and 2 mbar (b). Figure 3a.1 presents the same stability as the powder free acquisition of Fig. 2a, and the same was observed for lower pressures in the same conditions (not shown here). When increasing the pressure to 2 mbar, the SiH and H_2 Fulcher emission intensities show a different behavior at ignition. The emissions present a peak at ignition which is neither due to change in the RF power feed, nor in a change in RF matching (fixed position of capacitances). Moreover, the emissions are at steady-state ~2 seconds after ignition, which differs strongly compared to the case of Fig. 2b. Deeper analysis of the emission intensities shows (Fig. 3 a.2 and b.2) that the electron density varies also at ignition at 2 mbar, whereas it remains constant at 1.75 mbar. However, the intensity ratios of molecular hydrogen ($I_{\mathrm{Fulcher}}/I_{\mathrm{G0B0}}$) and atomic hydrogen ($I_{\mathrm{H}\alpha}/I_{\mathrm{H}\beta}$) in Figs. 3 a.3 and b.3 do not show a peak at ignition, meaning that the electron temperature remains stable. The peak in electron density can probably be associated to the formation of silicon clusters in the discharge [7,11] as soon as the discharge is ignited. First, the electron density is raised due to the electronic ionization by electron impact chain reaction, but as soon as the SiH_2 radical density is large enough, clusters are formed. Once formed, they accumulate negative charges on their surface, hence, reducing the electron density in the plasma. Further experiments have shown that the transition between these two regimes happens between 1.8 and 1.9 mbar with the used parameters. This suggests that the transition between clean discharge and discharge containing silicon cluster is very narrow. This correlates with static plasma experiments performed by Bano *et al* [6] showing that clusters are formed as soon as poly-silanes are produced in the discharge by SiH_2 and SiH_4 reaction.

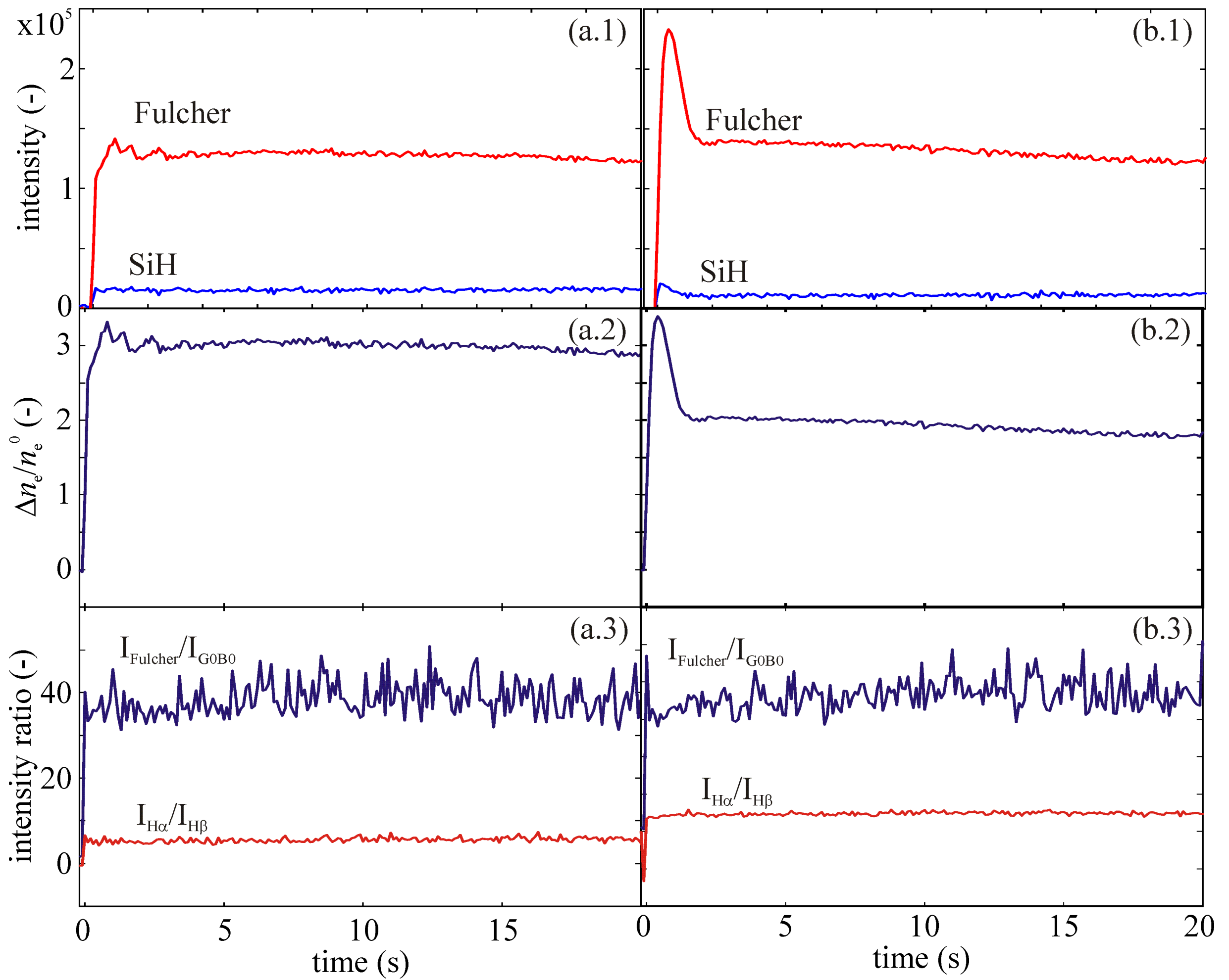

Figure 3: Emission intensities, electron density and hydrogen emission intensity ratio at ignition for a pressure of 1.75 mbar (a) and 2 mbar (b).

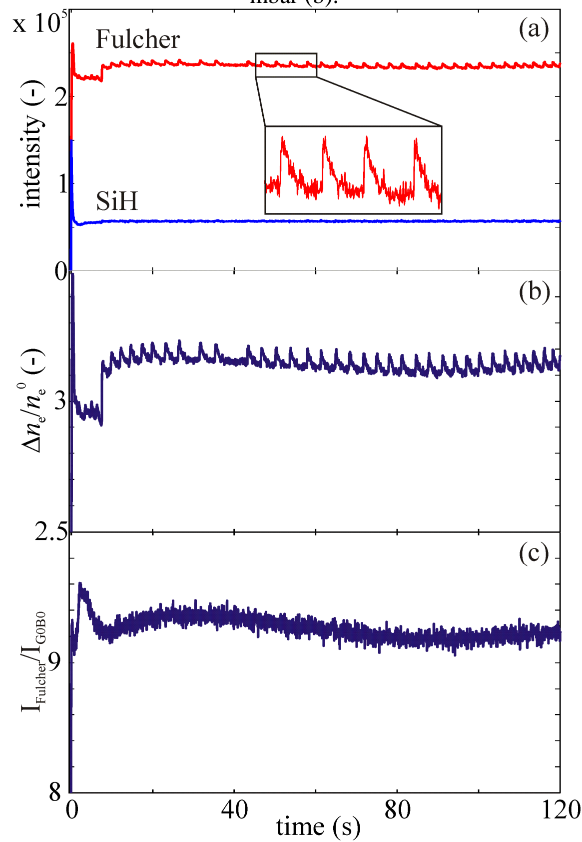

Figure 4: (a) SiH and H_2 Fulcher emission intensities, (b) electron density variation and (c) H_2 Fulcher over H_2 G_0B_0 emission ratio for a discharge performed with 4.5 mbar, 6.5 % of silane, and a RF power input of 1050 W.

Figure 4 presents the OES acquisition results for a deposition performed at higher silane concentration (6.6 %), higher pressure (4.5 mbar) and higher RF power input (1050W). Emission intensities show a spike at ignition as in the case at 2 mbar in Fig. 3b and a step after 5 seconds due to a change in the RF matching position. During steady-state power feed, i.e. after 5 seconds, small peaks with a frequency of about 1 Hz can be observed for both the SiH and the H_2 Fulcher emissions. Those can be associated to larger particles than small clusters discussed in Fig. 3 with cycle of growth and ejection out of the plasma [5,7]. First, small clusters are formed and due to their negative surface charge they are trapped within the plasma because of the drop of the electrical potential at the plasma boundary. While remaining in the plasma, their size increases due to silicon deposition and as soon as the drag force from the gas flow is large enough to compensate for the electrical repulsive force at the plasma boundary, the particles (no longer clusters) are expelled out of the discharge. When the particles are ejected, the electron density rises because of the absence of particles in the discharge until they appear and grow again, hence, reducing the electron density. The electron temperature does not show such oscillation, even if lower frequency (~0.01 Hz) oscillation can be observed.

Figures 3 and 4 have shown that even in the case of the presence of particles in the discharge the emission intensities are relatively constant or at least that the frequency of the oscillation induced by powder growth and ejection is stable. Figure 5 presents SiH and H_2 Fulcher emission intensities for a discharge in similar conditions that the one presented in Fig. 4, but with a slightly higher silane concentration (9.1 %). In this more favorable case for powder formation, we can observe first that the discharge is stable and after 20 seconds, oscillations can be observed as in the previous case. About 2 minutes after ignition, another behavior can be observed with cyclic transition from particle growth and ejection regime to powder free regime with constant emission intensities. Note that the transition from one regime to the other happens at a constant frequency.

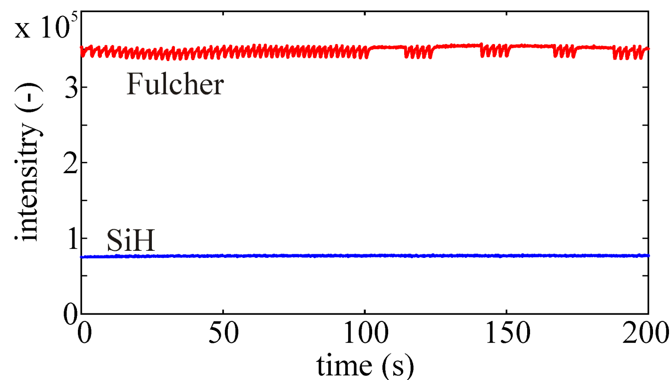

Figure 5: Example for a non-stable discharge with multiple oscillation frequencies.

To summarize, in this section it has been shown that time-resolved optical emission spectroscopy is able to detect powder formation in silane – hydrogen discharges. Moreover, different features can be observed and can be often associated to electron interaction with particle present in the discharge. The detection of powder necessitates only the observation of the silane and hydrogen emission intensities, but deeper investigation to extract the electron temperature and density variations is helpful to understand the mechanisms at the origin of powder formation.

3.2 Pressure series

In this section, a pressure series is presented with parameters suitable for the growth of microcrystalline silicon at high deposition rate. The parameters were a silane concentration of 13 % and a RF power of 1100 W:. Results of optical emission spectroscopy measurements are given in Fig. 6 with the SiH and H_2 Fulcher emission intensities (left column) and molecular ($I_{Fulcher}/I_{G0B0}$) and atomic ($I_{H\alpha}/I_{H\beta}$) hydrogen emission ratios (right column). We can observe that at 2 mbar the peak at ignition associated to cluster formation is already present and that until 4 mbar this is the only sign of particles formation in the plasma measurable by OES. While the pressure is increased, the dissociation efficiency of silane is increased due to the longer gas residence time in the discharge. The silane dissociation efficiency increase combined with the absence of powder between 2 to 4 mbar (even if clusters are present) results in an increase in the deposition rate from 0.79 to 1.16 nm/s has shown in Fig. 7. When increasing the pressure to 4.5 mbar, OES shows that coarser particles are present in the discharge and are ejected out of the plasma volume with a frequency of about 1 Hz. As shown in Fig. 7, the use of silane radicals to form powder particles that are pumped out makes the deposition rate lower because less silane radicals contribute to the film growth. When increasing the pressure to higher values, the cycles of powder growth and ejection are still observable even if less pronounced. Moreover, the behavior at ignition becomes more chaotic with different time variation between SiH and H_2 emission suggesting the presence of large particles which is confirmed by the reduction in signal intensity due to deposition of powder particles on the view-port window. For very high

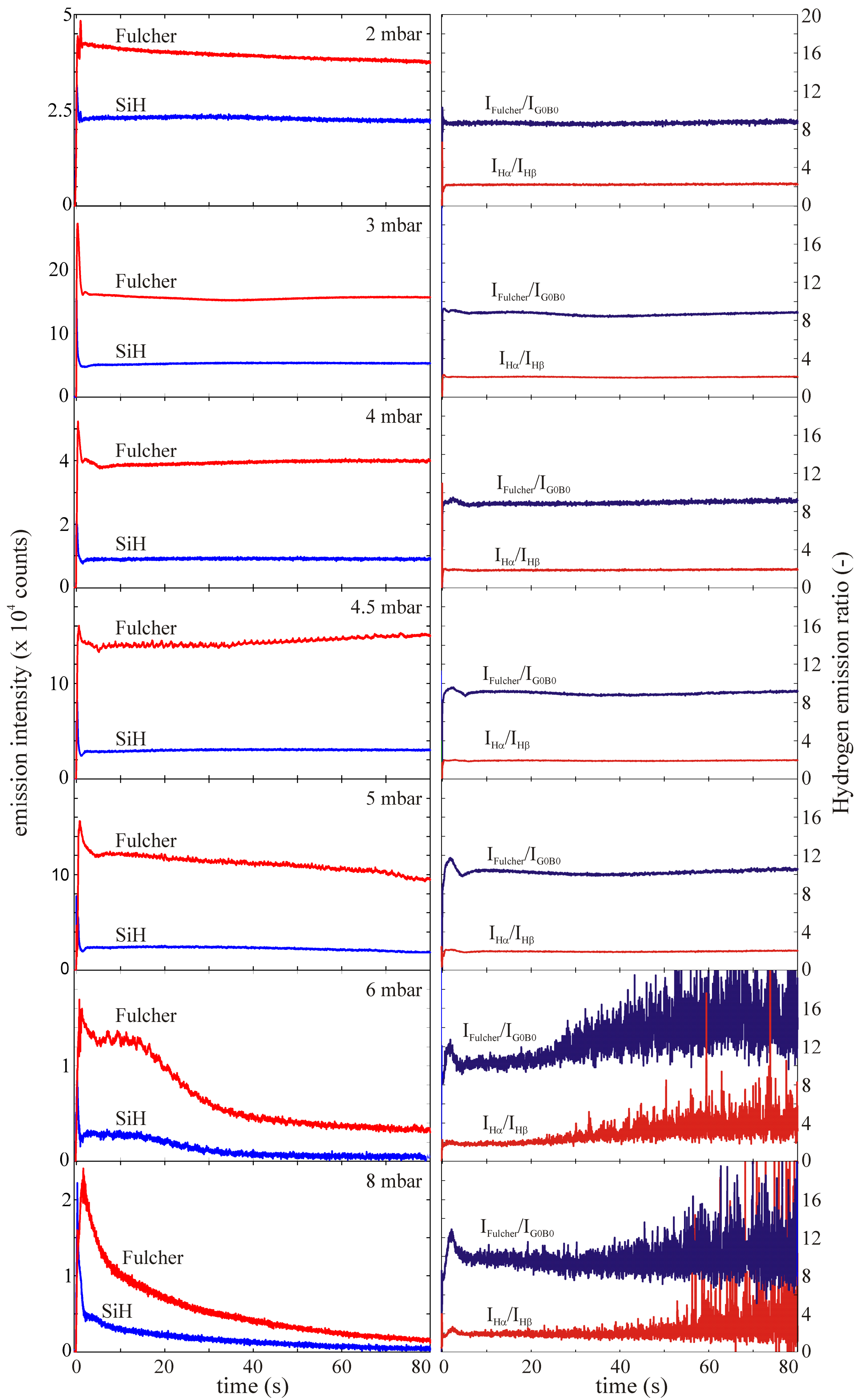

Figure 6: OES results for a pressure series with c=13 % and RF power of 1100 W.

pressures – 6 and 8 mbar – the emission intensities are even more affected at ignition and rapid decrease in silane intensity confirm the presence of coarse powder in the plasma. Moreover, the electron temperature becomes very unstable with strong oscillations at frequency smaller than the integration frequency (1/0.025=40 Hz). The strong formation of powder particle in these cases has for effect to reduce drastically the deposition rate that falls back to 0.74 nm/s as shown in Fig. 7.
These results show that the electron temperature is less affected than the electron density by powder formation in the discharge. However, the right-hand side column of Fig. 6 shows that compared to powder free discharge (2 mbar), powdery discharges presents variation of the electron temperature during the 5 seconds following the plasma ignition. Therefore, this feature can also be used to detect if powder is formed or not in the discharge.

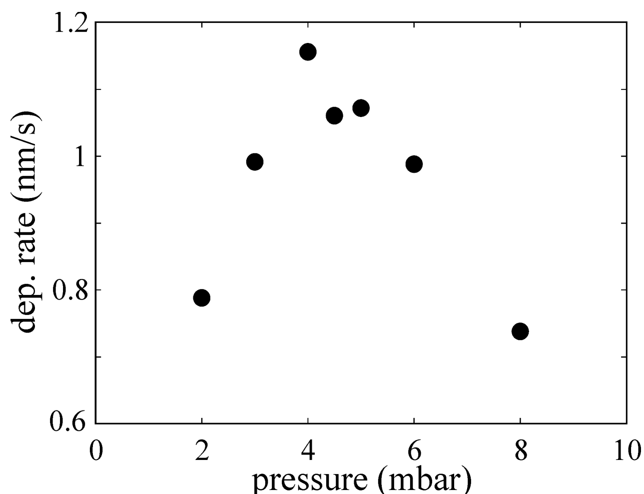

Figure 7: Deposition rate as a function of the working pressure with the same parameters as in Fig. 6.

4. CONCLUSIONS

Time-resolved optical emission spectroscopy (OES) was used to detect the presence of powder formation in silane-hydrogen discharge in large area plasma-enhanced chemical vapor deposition reactor. It was shown that this technique was suitable to detect different regimes of powder formation between the two extreme cases where the discharge is free of powder and discharge leading to strong dust formation. The first sign of powder formation can be observed even at very low pressure, RF power and silane concentration and can be attributed to silicon cluster produced directly after the discharge ignition. For discharge more favorable to powder formation, i.e. at higher pressure, RF power or silane concentration, cycle of particle growth and ejection out of the discharge can also be observed by OES. It was shown that powder has more influence on the electron density than on the electron temperature. However, the electron temperature becomes very unstable when strong dust formation is observed. Finally, it was shown that as soon as cycles of powder growth and ejection are observed, the deposition rate drops because of the loss of silicon radicals for deposition onto the substrate.

Acknowledgments

This work was founded by the Swiss Federal Office for Energy and by Swiss Electric Research.

References

[1] Ross, R.C. and Jaklik Jr., J. , “Plasma polymerization and deposition of amorphous hydrogenated silicon from rf and dc plasmas”, J. Appl. Phys. 55(10), 3785-3794 (1983).
[2] Strahm, B., Howling, A.A., Sansonnens, L., Hollenstein, Ch., Kroll, U., Meier, J., Ellert, Ch., Feitknecht, L. and Ballif, C. , “Microcrystalline silicon deposited at high rate from pure silane with efficient gas utilization“, Solar Energy Mater. Solar Cells 91, 495-502 (2007).
[3] Rech, B., Roschek, T., Repmann, T., Müller, J., Schmitz, R. and Appenzeller, W. , “Microcrystalline silicon for large area thin film solar cells“, Thin Solid Film 427, 157-165 (2003).
[4] Gallagher, A. , ”Neutral radical deposition from silane discharges”, J. Appl. Phys. 63(7), 2406-1413 (1988).
[5] Johnson, E.V., Djeridane, Y., Abramov, A. and Roca i Cabarrocas, P. , ”Experiment and modeling of very low frequency oscillations in RF-PECVD: a signature for nanocrystal dynamics”, Plasma Sources Sci. Technol. 17, 035029 (2008).

[6] Bano, G., Horvath, P., Rozsa, K. and Gallagher, A. , ”The role of higher order silane in silane-discharge particle growth”, J. Appl. Phys. 98, 013304 (2005).
[7] Stoffels, W.W., Stoffels, E., Kroesen, G.M.W. and de Hoog, F.J. , “Electron density fluctuations in a dusty Ar/SiH_4 rf discharge“, J. Appl. Phys. 78(8), 4867-4872 (1995).
[8] Nunomura, S., Yoshida, I. and Kondo, M. , ”Time-dependent gas phase kinetics in a hydrogen diluted silane plasma”, Appl. Phys. Lett. 94, 071502 (2009).
[9] Howling, A.A., Strahm, B., Colsters, P., Sansonnens, L. and Hollenstein, Ch. , “Fast equilibration of silane/hydrogen plasmas in large area RF capacitive reactors monitored by optical emission spectroscopy“, Plasma Sources Sci. Technol. 16, 679-696 (2007).
[10] Fantz, U. , ”Spectroscopic diagnostics and modeling of silane microwave plasmas”, Plasma Phys. Controlled Fusion 40, 1035-1056 (1998).
[11] Boufendi, L. and Bouchoule, A. , ”Particle nucleation and growth in a low-pressure argon-silane discharge”, Plasma Sources Sci. Technol. 3, 262-267 (1994).